SASEC2015
Third Southern African Solar Energy Conference
11 – 13 May 2015
Kruger National Park, South Africa

A NOVEL COMPUTATIONAL APPROACH TO THE COMBINE OPTICAL AND THERMAL MODELLING OF A LINEAR FRESNEL COLLECTOR RECEIVER

Moghimi, M.A., Craig, K.J.* and Meyer J.P.
*Author for correspondence
Department of Mechanical and Aeronautical Engineering,
University of Pretoria, Pretoria, 0002,South Africa,
E-mail: ken.craig@up.ac.za

ABSTRACT

A computational approach is presented that uses the finite volume (FV) method in the Computational Fluid Dynamics (CFD) solver ANSYS Fluent to perform both the ray tracing required to quantify the optical performance of a line-concentration Linear Fresnel Collector (LFC) receiver, as well as the conjugate heat transfer modelling required to estimate the thermal efficiency of such a receiver. It is shown that the Discrete Ordinates method can provide an accurate solution of the Radiative Transfer Equation (RTE) if the shortcomings of its solution are addressed appropriately in the FV CFD solver. This approach is evaluated for a 2-D sample test case that includes a 2-D LFC optical domain of which the results are compared to those obtained with the Monte Carlo ray tracer, SolTrace. The outcome of the FV ray tracing in the LFC optical domain is mapped as a non-uniform heat flux distribution in the 3-D cavity receiver domain and this distribution is included in the FV conjugate heat transfer CFD model as a volumetric resource. The result of this latter model is the determination of the heat transferred to the heat transfer fluid running in the collector tubes, thereby providing an estimation of the overall thermal efficiency. To evaluate the effectiveness of the phased approach, the 2-D:3-D approach is compared to results of a fully integrated, but expensive, 3-D optical and thermal model. It is shown that the less expensive model provides similar results and that it provides the benefit of working in one simulation environment, i.e., ANSYS Workbench, where additionally optimization studies can be performed in future work.

INTRODUCTION

One of the traditional approaches to determining the thermal efficiency of linear Concentrated Solar Power (CSP) plants, whether one with parabolic trough collectors (PTCs) or Linear Fresnel Collectors (LFCs), is to model the solar load using a ray tracer, of which the Monte Carlo method is the most common [1]. The resulting absorbed solar irradiation is then applied as a boundary condition in a Computational Fluid Dynamics (CFD) model to determine the conjugate heat transfer that involves mechanisms like conduction, natural and forced convection, as well as thermal re-radiation. LFCs are the focus of this paper as they still have to be fully exploited through optimization. Previous researchers have performed optimization studies that either included economic factors as well [2] or that only focus on thermal and optical performance parameters [3, 4]. The use of different software tools for optics and thermal performance means that a single simulation-optimization environment where parameterized models can be fully integrated remains a challenge. The current study therefore illustrates the use of the ANSYS Workbench environment, where the geometry, meshing, CFD solution and optimization tools (DesignXplorer) are all linked through parameters, to perform both the optical and thermal evaluation of the receiver within a mirror field. If illustrated to be cost-effective and accurate, the environment can then be used in optimization studies, as performed, e.g., in Moghimi, *et al.* (2014) [5]. Therefore, using the FV method in commercial CFD codes for ray tracing and proving it to be an accurate tool for calculating the solar load on the heat transfer fluid (HTF) in a solar application is a large challenge that has not been done before to the best of the authors' knowledge. If successful, the approach paves the way for using the integrated optimization platform of ANSYS Workbench to perform comprehensive optimization studies of a CSP domain.

In this paper, after an introduction discussing the defects of the finite volume (FV) and Discrete Ordinates (DO) method for solving the Radiative Transfer Equation (RTE), the accuracy of the optical simulation method is illustrated for a simple test case from literature. The lessons learnt in this case study are then applied to a more complex solar implementation and the results are compared with those using a SolTrace [6] model to see if the FV shortcomings can be mitigated in a complex solar geometry scenario. After assurance is obtained of the accuracy of the FV optical results, this paper introduces a new cost-effective sequential method that uses an FV optics modelling in 2-D and then maps the results on a 3-D cavity thermal domain.

As proof of the validity of the sequential approach, it is compared to an expensive full 3-D model of the entire collector (mirror filed and cavity) to illustrate both the cost-effectiveness and accuracy. The solar implementation used in this paper is the mirror field layout and receiver position of the FRESDEMO [2, 7] project.

NOMENCLATURE

k	[J/kg]	Turbulent kinetic energy
l	[m]	Mixing length
N	[-]	Number
r	[m]	Location of annulus element from the pipe centre
R	[m]	Pipe inner diameter
T	[K]	Local temperature
v_z	[m/s]	Velocity in z direction
c, d, e, f, H, m, p, t, w, W, ID, a'	[m]	Geometrical parameters shown in Figure 3

Special characters

ε	[J/kgs]	Turbulence dissipation rate
μ	[Ns/m^2]	Dynamic viscosity
θ_1, θ_2	[degree]	Angular parameters shown in Figure 3
ρ	[kg/m^3]	density
τ_w	[N/m^2]	Wall shear
$V_{centerline}$	[m/s]	Maximum velocity value in a pipe cross section

Subscripts

θ	Angular direction	N	Number of ordinate directions
ϕ	Angular direction	z	Cartesian axis direction

FV SOLUTION OF RTE USING DO

The determination of the non-uniform solar heat flux distribution around the absorber tubes of an LFC cavity is one of the main purposes of the optical modelling that requires the solution of the RTE. Two of the well-known solution methods of the RTE is the Implicit Monte Carlo (IMC) and DO methods. The IMC which is the foundation of most ray-tracing software yields very accurate results when simulating enough particles but can become processor and memory intensive at high ray counts. The DO method on the other hand is easy to implement in FV, and easy to solve especially in serial calculations. In addition, the DO method determines the solution of the RTE on the same mesh as the energy, mass and momentum conservation equations which leads to a close coupling of surface temperature and radiative energy. This implies that the DO can be applied to complex geometries for different participating media such as non-gray, anisotropically scattering, non-isothermal, absorbing, and emitting media. Nevertheless, the DO method has two major shortcomings due to its FV nature, namely the "false scattering" and "ray effect" [9]. The first causes smearing of the propagated radiation while the second causes an incorrect direction of the wave front.
These shortcomings and theirs effects on final results could be the reason why researchers use ray-tracing software instead of FV in their studies. In the following ways are investigated that illustrate how these shortcomings can be mitigated in commercial FV codes (ANSYS Fluent [10], an FV CFD solver) through testing the method on a simple test case.

The RTE in ANSYS Fluent is solved with the S_2 method, a subset of the Discrete Ordinates (DO) using the S_N approach, where N is number of ordinate directions. The angular space is subdivided into $N_\theta \times N_\phi$ control angles, each of which is further subdivided by pixels. For 1-D, $2 \times N_\theta \times N_\phi$ directions of the RTE equations are solved, for 2-D, $4 \times N_\theta \times N_\phi$ directions, while for 3-D, $8 \times N_\theta \times N_\phi$ directions are computed.

The suggestions for mitigating the shortcomings of the FV DO method, are: refining the mesh; increasing the number of angular discretizations; and increasing the order of the spatial discretization of the DO method.

A test case to evaluate the effect of false scattering as well as the so-called ray effect is presented in Figure 1 [11,12].

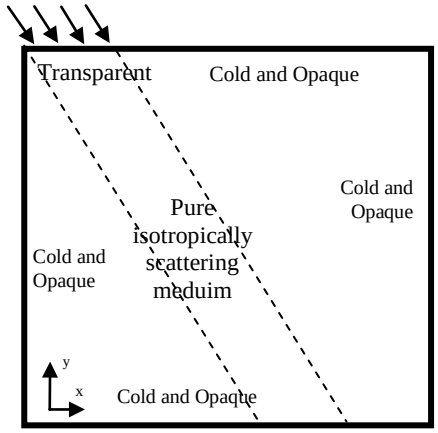

Figure 1 Oblique collimated radiation test case

For this domain, the effect of varying the mesh density, then increasing the angular discretization divisions, changing the discretization order and lastly combining the optimal combination of these settings is illustrated in Figure 2 when using ANSYS Fluent. In Figure 2a, the ray effect due to an insufficient number of angular discretizations is obvious, as the focus of the incoming oblique ray misses the intended target as illustrated by the comparative accurate Monte Carlo ray-tracing solution. The reduction in the smearing of the wave front is noted as the mesh is refined (Figure 2b) but the sharp discontinuity in absorbed radiation is not captured, even for the finest mesh. Second-order discretization improves the smearing in a marked fashion (Figure 2c), while the optimal combination (Figure 2d) provides the sharp features at the impact location also exhibited by the Monte Carlo solution.

LFC OPTICAL FV SOLUTION COMPARED WITH SOLTRACE

Having proven that the FV shortcomings can be reduced by a wise choice of CFD solver settings in a simple test case, a complex solar applications is now considered to investigate if the accuracy can be maintained. Therefore, an optical domain of a linear solar collector, an LFC domain, is investigated with FV and compared with a Soltrace solution. The chosen LFC optical domain and its dimensions are shown in Figure 3 and Table 1. The computational domain used in the CFD FV implementation is shown in Figure 4.

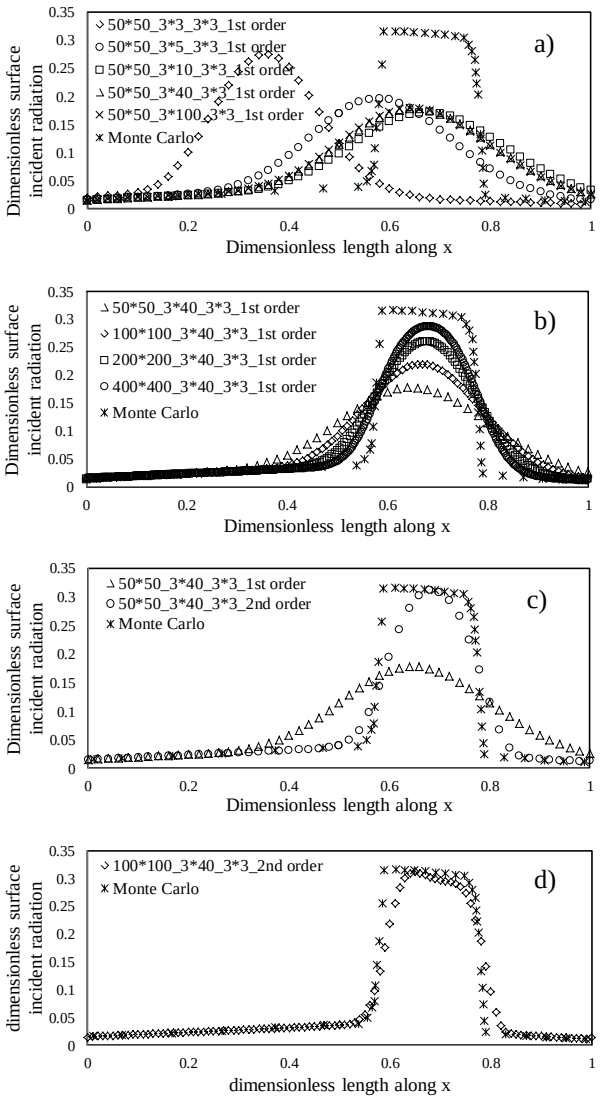

Figure 2 Variation of a) angular discretization, b) mesh density, c) discretization order, d) optimal combination of settings; for oblique collimated radiation test case, as compared with Monte Carlo solution [11,12]

To confirm the correct settings for angular discretizations and mesh refinement, a study was done of which the results are displayed in Figure 5. It can be seen that an $N_\theta \times N_\phi$ of 3x200 and a mesh of 347k cells gives sufficient resolution for an independent solution. The incident radiation contours for this case are displayed in Figure 6. Note that the blocking and shading effect of the receiver and adjacent mirrors can clearly be seen, as well as the concentration effect of the mirror field on the receiver. The case shown is for a Direct Normal Irradiation of 1000 W/m^2 entering the domain vertically. Contrary to the collimated radiation in the test case above, the beam angle corresponded to the subtended angle of the sun at 9 mrad or 0.53°. The material properties and boundary used in the CFD 2-D optical model are given in Tables 2 and 3, respectively.

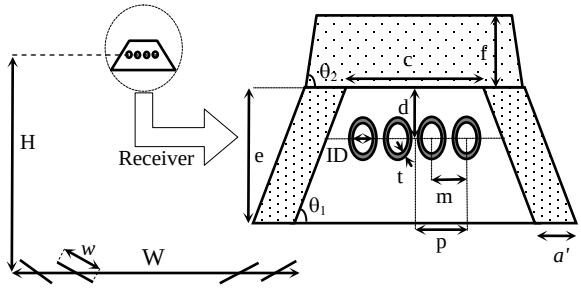

Figure 3 Schematic layout of the LFC mirror field and receiver

Table 1 Dimensions of the LFC mirror field and receiver

Number of primary mirrors	25	Pipe thickness (t [mm])	5	Pipe offset (d [mm])	55
Solar field width (W [m])	21	Pipe ID (ID [mm])	40	Pipe offset from each pipe (m [mm])	75
Primary mirror width (*w* [m])	.6	Cavity top side width (c [mm])	400	Outer pipe centre (p [mm])	112.5
Receiver height (H [m])	8	Cavity depth (e [mm])	240	Top insulation thickness (f [mm])	85
Side insulation thickness (*a'* [mm])	40	θ_1	30°	θ_2	60°

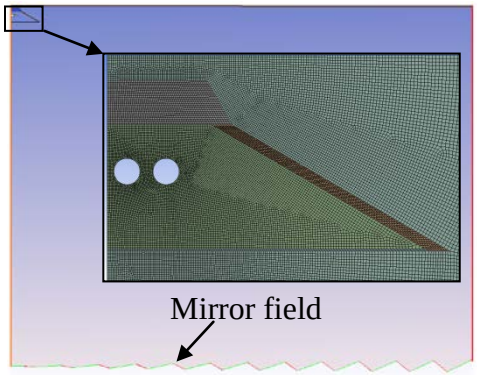

Figure 4 CFD domain with receiver insert showing mesh

To validate the FV result, a SolTrace [6] model was constructed with sample rays obtained depicted in Figure 7. A Gaussian sun shape with the width of 2.63 mrad was used. The glass thickness is included with a refraction coefficient of 1.5. The glass is set not to absorb any radiation. The tube reflectivity was set at 0.04 while that of the cavity walls were set at 0.95 as for the FV model.

The comparison between the Monte Carlo (SolTrace) and the FV CFD results is shown in the form of circumferential distributions around the 3rd and 4th pipe of the absorbed radiation flux in Figure 8. For the comparison, the glass was without absorption in the CFD model. Two FV results for a coarser mesh and fewer angular discretizations are also shown to illustrate the reduction in false scattering and ray effect with increasing resolution. A ray count sensitivity study was done for SolTrace (not reported here) to determine that a ray intersection count of 1 million (requiring more than 4 million released rays) gave both a symmetric and fairly even distribution of absorbed power. It can be seen that the agreement between the Monte Carlo and FV method is good, giving confidence that the FV method can predict both the

integrated as well as detail absorbed radiation distributions accurately.

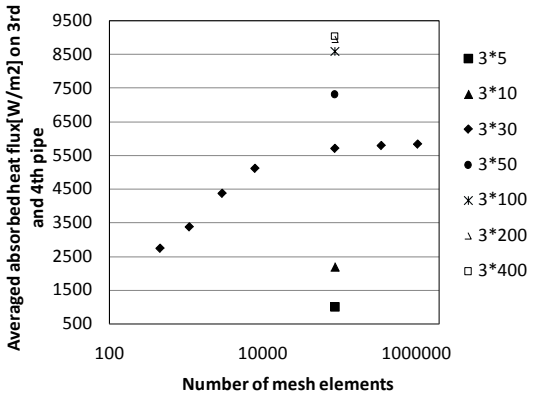

Figure 5 Mesh and angular discretization refinement study

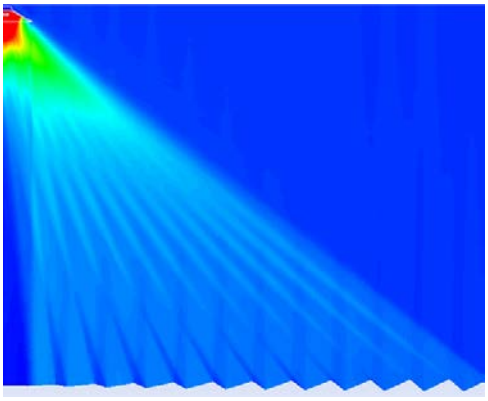

Figure 6 Incident radiation contours obtained by the CFD FV method (347k mesh, DO $N_\theta \times N_\phi$ =3x200)

Table 2 Material properties used in 2-D CFD FV simulation

Material	Participating in radiation	Absorption coefficient [m^{-1}]	Refractive index	Other
Solid Air in and around cavity	Yes	0	1	Thermal conductivity = .0242 [W/m-K], Specific heat=1006.43 [J/kg-K], Density=1.225 [kg/m^3]
Semi-transparent glass	Yes	106	1.5	Thermal conductivity = 1.5 [W/m-K], Specific heat=786 [J/kg-K], Density=2650 [kg/m^3]
Insulation-glass wool	No	0	1	Thermal conductivity = piecewise-linear [W/m-K], Specific heat=446 [J/kg-K], Density=48 [kg/m^3]

LFC CAVITY RECEIVER THERMAL MODELLING IN ANSYS FLUENT

The LFC cavity was modelled in 3-D in order to capture the transfer of the solar load in the cavity receiver (as obtained in the 2-D FV solution) to the heat transfer fluid (HTF). A dual-band grey radiation model was used as in [5]. A 1-cm length of pipe was considered with 5 computational cells. The computational domain with an insert of the mesh for the HTF is shown in Figure 9. Note that a thin shell of the pipe is modelled separately for the application of the volumetric heat source.

The material properties and boundary conditions are listed in Tables 4 and 5. The velocity and turbulent profiles at inlet of domain comply with the formulae in equations (4) to (7).

$$\frac{v_z}{V_{centerline}} = \left(1 - \frac{r}{R}\right)^{\frac{1}{7}} \tag{4}$$

$$\frac{\tau_w}{\rho} = 0.0225 \times V_{centerline}^2 \times \left(\frac{\rho V_{centerline} R}{\mu}\right)^{\frac{-1}{4}} \tag{5}$$

$$k_{near-wall} = \frac{v_\tau^{\,2}}{\sqrt{C_\mu}} \;\&\; k_{free\_stream} = 0.002 V_{centerline}^2 \tag{6}$$

$$\varepsilon = \frac{C_\mu^{3/4}\left(k^{3/2}\right)}{l} \tag{7}$$

Table 3 Boundary conditions for 2-D CFD FV simulation

Surface	BC type	Thermal Condition	Temperature [K]	Emissivity	Other
Solar field top side	Semi-transparent	Constant Temperature	1	1	Beam width $\theta = 0.53^\circ$ & $\phi = 0.53^\circ$, Direct Irradiation=1000 [W/m^2]
Domain side and gaps between mirrors	Opaque and black body	Constant Temperature	1	1	-
Mirrors	Opaque and purely reflective	Constant Temperature	1	0	-
External surfaces of insulation	opaque	Constant Temperature	1	1	-
Cavity walls	Opaque and reflective	Constant Temperature	1	.05	-
Glass sides	Semi-transparent	Coupled	-	0	-
Outer surface of pipes	Opaque with selective coating	Constant Temperature	1	0.95	-

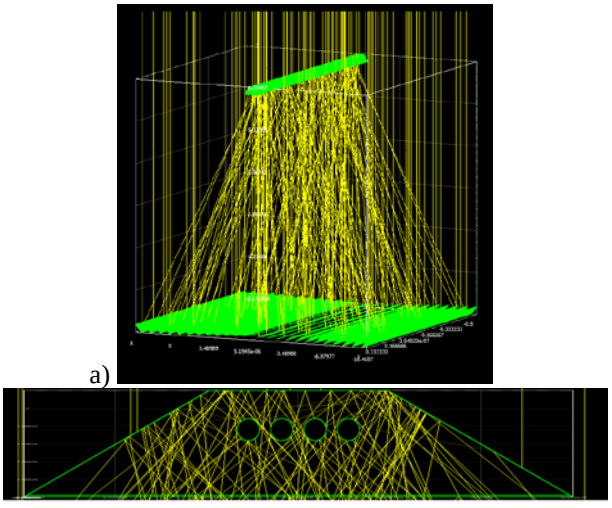

Figure 7 SolTrace model of LFC a) mirror field and b) close-up of receiver

The non-uniform solar heat flux on an absorber tube as calculated in the 2-D CFD FV solution (Figure 8) was patched onto the 3-D domain by using the following procedure [13]:

1. Convert absorbed radiation (solar load) on collectors into interpolation file
2. Define User-defined scalar (UDS)

3. Interpolate data to UDS
4. Copy UDS to User-Defined Memory (UDM) using User-Defined Function (UDF)
5. Assign source term using UDF to patch load as volumetric heat source

The result of the procedure is shown in Figure 10 in the form of UDM contours on the tube surface.

The temperature contours on the outlet plane of the cavity is shown in Figure 11 for two cases.

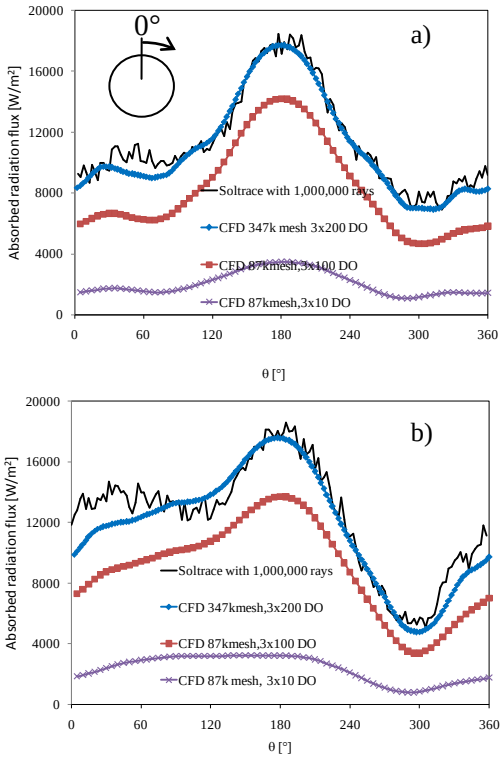

Figure 8 Comparison of SolTrace (1000000 rays) and CFD FV absorbed radiation flux around circumference of a) 3rd and b) 4th pipe in LFC receiver

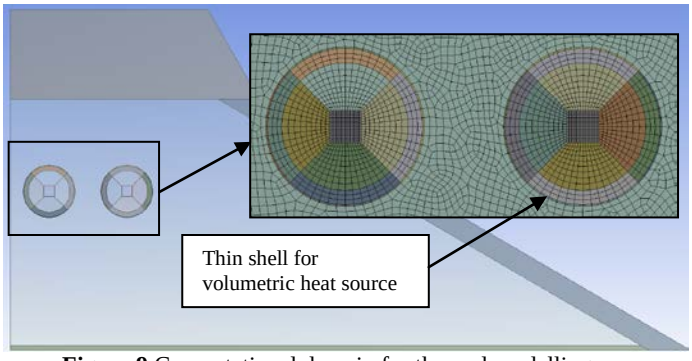

Figure 9 Computational domain for thermal modelling

In Figure 11a, the air in the cavity is considered as solid, i.e., only the energy and DO equations are solved. In Figure 11b, the air is modelled as an incompressible ideal gas and gravity is enabled, so that natural convection can occur. For this cavity configuration, the natural convection does not have a significant effect on the minimum temperatures for the two cases (287.96 K versus 288.20 K). The additional cooling effect of the moving air reduces the maximum temperature from 312.22 K to 311.08 K.

Table 4 Material properties used in 3-D CFD thermal simulation

Material	Density [kg/m^3]	Specific heat [J/kg-K]	Thermal conductivity [W/m-K]	Other
Air in cavity	Incom-pressible ideal gas	*f*(T) piece-wise	*f*(T) piece-wise	Viscosity [Pa.s]: piece-wise *f*(T), Participating in radiation
Glass	2650	786	1.5	Refractive index = 1.5, absorption coefficient [m^{-1}] = 2300, Participating in radiation
HTF-water	998	4182	0.6	Viscosity [Pa.s]= 0.001003
Insulation-glass wool	48	446	*f*(T)	-
Pipe-carbon steel	7818	670	54	-

Table 5 Boundary conditions for 3-D CFD thermal simulation

Surface	BC type	Temperature [K]; Heat transfer coefficient [W/m^2-K]	Emissivity
Pipe inner side	Coupled thermal wall	-	-
Pipe outer side	Coupled thermal wall, opaque with selective absorber coating	-	$Band_0$= 0.95, $Band_1$= 0.1
Top and side wall	Coupled thermal wall, opaque with reflective coating	-	$Band_0$= 0.05, $Band_1$= 0.05
Glass inner side	Coupled thermal wall, Semi-transparent	-	-
Glass outer side	Mixed thermal condition	300 (T_{conv}); 5 305 (T_{rad})	0.9
Insulation outer side	Mixed thermal condition	300 (T_{conv}); 5 T_{sky} =0.0522* 300$^{1.5}$ (T_{rad})	0.75
Pipe	Fully developed turbulent velocity inlet (UDF (u,k,ε)), pressure outlet	300	-

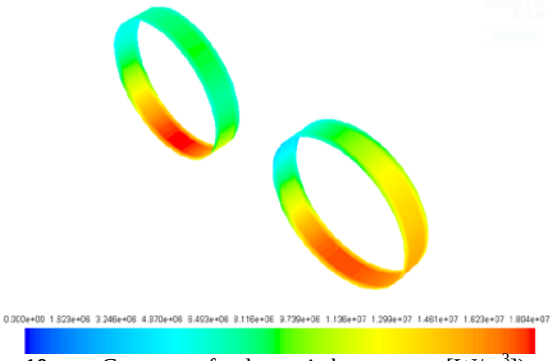

Figure 10 Contours of volumetric heat source [W/m^3]) on pipe surface

To validate the phased approach outcome and to check the accuracy of the data interpolation in the sequential approach (2-D FV optical solution followed by a 3-D FV CFD thermal solution), the same solar field and cavity was modelled fully in a 3-D model. The computational domain is shown in Figure 12. The full approach is much more expensive, because all the equations (mass, momentum and energy) are solved in the whole 3-D domain, and the DO method requires $8\times N_\theta \times N_\phi$ ordinate directions and needs to be solved for 5 computational cells in the third dimension. In comparison, the 2-D optical model requires only $4\times N_\theta \times N_\phi$ ordinate directions and only solves the DO and energy equations, while the 3-D thermal model (where the mass, momentum and energy equations are solved) is restricted to the cavity only. The material properties

and boundary conditions of this model are the same as for the above models. When using a DO setting of 3x30 and 5 computational cells in the HTF flow direction, the results in Table 6 were obtained. The agreement is within 4% emphasizing the power of the much less expensive phased approach.

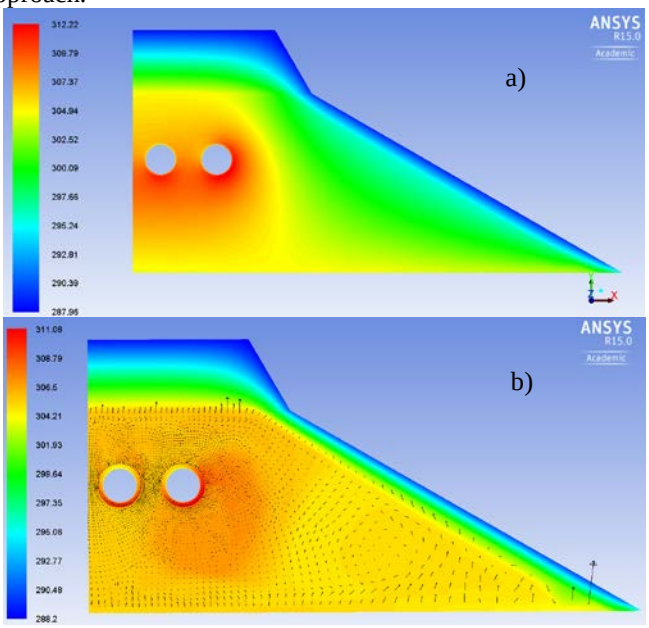

Figure 11 Temperature contours for a) Solid air in cavity, b) Natural convection in cavity overlaid with velocity vectors

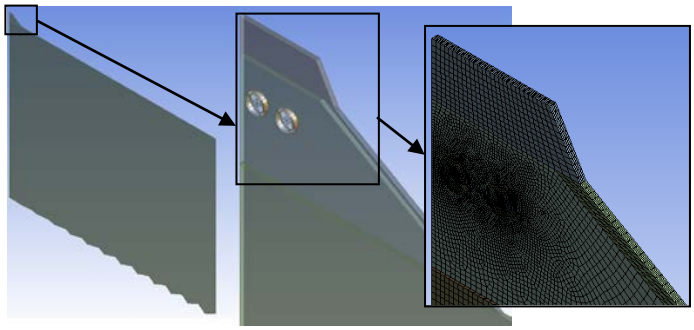

Figure 12 Full 3D optical and thermal CFD domain

CONCLUSIONS

This paper has illustrated a novel, cost-effective and accurate approach to combine the optical and thermal evaluation of a Linear Fresnel Collector cavity receiver for a specific mirror field in one CFD environment. It was shown that the ANSYS Fluent and Workbench environment can be used to accurately model the radiation transport with a finite volume method by comparing it to a Monte Carlo ray-tracing method using SolTrace. The result of the radiation model was then incorporated into a 3-D CFD thermal model where conduction, natural convection and thermal re-radiation were solved using a grey dual-band approach. The temperature rise in the heat transfer fluid is compared to that of a separate expensive 3-D model that included both the optical and thermal solution and results within 4% were achieved, validating the approach. Therefore, this approach could be easily extended to other solar fields or used in their optimization process by future researchers.

Table 6 Comparison between 2-D optical/3-D thermal and full 3-D optical and thermal model

		Tin [K]	Tout [K]	HTF Inlet Energy [W]	HTF Outlet Energy [W]	Total Energy transferred to HTF [W]
2-D optical, 3-D thermal model	3rd pipe	300	300.01245	1224.4753	1232.7577	8.2824
	4th pipe	300	300.01428	1224.473	1233.9722	9.4992
	total					**17.7816**
Full 3D optical and thermal model	3rd pipe	300	300.01309	1222.5682	1230.3471	7.7789
	4th pipe	300	300.01477	1220.7763	1231.4577	10.6814
	total					**18.4603**

ACKNOWLEDGEMENTS

The authors would like to acknowledge the support from the University of Pretoria (South Africa) and the South African National Research Foundation (DST-NRF Solar Spoke).

REFERENCES

[1] Bode, S.J. and Gauché, P., Review of optical software for use in Concentrated Solar Power systems. SASEC 2012, 21-23 May, 2012, Stellenbosch, South Africa.

[2] Mertins, M., Technische und wirtschaftliche Analyse von horizontalen Fresnel-Kollektoren, PhD thesis, 2009, Universität Karlsruhe.

[3] Morin, G., Platzer, W., Eck, M., Uhlig, R., Häberle, A., Berger, M., and Zarza, E., Road map towards the demonstration of a Linear Fresnel Collector using a single tube receiver, 13th International Symposium on Concentrated Solar Power and Chemical Energy Technologies, SolarPACES 2006, Seville, Spain.

[4] Montes, M.J., Abbas, R., Rovira, A., Martínez-Val, J.M., and Muñoz-Antón, J., Analysis of Linear Fresnel Collector designs to minimize optical and geometrical losses, SolarPACES 2012, Marrakesh, Morocco.

[5] M.A. Moghimi, K. Craig and J.P. Meyer, Optimization of a trapezoidal cavity absorber for the Linear Fresnel Reflector, SASEC 2014, 27-29 January, 2014, Port Elizabeth, South Africa.

[6] SolTrace, National Renewable Energy Laboratory, www.nrel.gov/soltrace.

[7] Bernhard, R., Laabs, H.-G., de Lalaing, J., Eck, M., Eickhoff, M., Pottler, K., Morin, G., Heimsath, A., Georg, A. and Häberle, A., Linear Fresnel Collector demonstration on the PSA Part 1 – Design, construction and quality control, 14th International Symposium on Concentrated Solar Power and Chemical Energy Technologies, SolarPACES 2008, Las Vegas, USA.

[8] Modest M.F., Radiative Heat Transfer, Elsevier, Third edition, 2013.

[9] Chai, J.C. and Patankar, S.V., Discrete-ordinates and finite-volume methods for radiative heat transfer, chapter in Handbook of Numerical Heat Transfer, 2nd Ed., , John Wiley & Sons, 2006.

[10] ANSYS Fluent Theory Guide, ANSYS v.14,5, 2013.

[11] Li H., Reduction of false scattering in arbitrarily specified discrete directions of the discrete ordinates method, Journal of Quantitative Spectroscopy & Radiative Transfer, Vol. 86,2004, pp. 215–222.

[12] Hachicha, A.A., Numerical modelling of a parabolic trough solar collector, PhD Thesis, 2013, Universitat Politècnica de Catalunya.

[13] Craig, K.J., Harkness, A.W., Kritzinger, H.P. & Hoffmann, J.E., Analysis of AP1000 reactor vessel cavity and support cooling, Paper ECN2010-A0459, European Nuclear Conference (ENC2010), 30 May - 2 June 2010, Barcelona, Spain.